Characterizing Human Body Shadowing at 32.5 GHz Through Cylindrical Diffraction Theory

Ahmed Alabish
dept. Computer Science
Libyan Academy
Zawia, Libya
ahmed.cs@academy.edu.ly

Tahanie Hamead
dept. Computer Science
Libyan Academy
Gharyan, Libya
Samataha.ramahame@gmail.com

Manal ghoumah
dept. Computer Science
Libyan Academy
Mislata, Libya
manalgoma90@gmail.com

Mahmoud Abdullah
Science Faculty,dept.Computer Science, University of Zawia
Zawia, Libya
m.abdullah@zu.edu.ly

Abstract— The advent of 5G networks has revolutionized wireless communications by unlocking unprecedented data rates through millimeter-wave (mmWave) frequencies. However, the short wavelengths of mmWave signals (e.g., 32.5 GHz) make them highly vulnerable to obstructions, particularly human blockage, posing significant challenges for reliable link prediction and network planning. Existing models often oversimplify human-induced attenuation, limiting their accuracy in real-world scenarios. This work addresses this gap by proposing a cylindrical diffraction model to quantify human blockage effects at 32.5 GHz—the first application of such a model at this frequency. Through controlled experiments, we measured signal degradation as a human subject progressively blocked a 2-meter mmWave link, revealing a sharp decline in received power from −41.2 dBm (no blockage) to −69.7 dBm (full blockage). The cylindrical model demonstrated strong alignment with empirical trends, accurately capturing the nonlinear increase in attenuation as the human approached the line-of-sight path. Notably, the model matched baseline measurements within 1.4 dB and predicted full-blockage loss within 7 dB of observed values, despite inherent simplifications. This study underscores the efficacy of cylindrical modelling for mmWave blockage prediction while highlighting critical refinements needed for practical deployment, such as incorporating material properties and antenna radiation patterns. By bridging theoretical and empirical insights, our work provides a foundational framework for enhancing 5G/6G network resilience in human-dense environments, ensuring robust performance for high-data-rate applications.

Keywords — 5G/6G, millimeter-wave, human blockage, cylindrical model, empirical validation.

I. INTRODUCTION

The fifth-generation (5G) wireless technology has revolutionized global connectivity by delivering unprecedented data rates exceeding 20 Gbps and ultra-low latency as low as 1 millisecond, enabling transformative applications such as autonomous vehicles, augmented reality (AR), and industrial automation [1, 2]. These advancements are underpinned by the adoption of millimeter-wave (mmWave) frequencies (24–100 GHz), which offer vast bandwidth but face significant propagation challenges due to their short wavelengths (e.g., 9.2 mm at 32.5 GHz) [3, 4]. While mmWave technology addresses the escalating demand for high-speed data transmission, its susceptibility to signal attenuation, blockage, and environmental interference necessitates advanced modeling techniques to ensure reliable network performance [5, 6].

A critical challenge in mmWave systems lies in accurately modeling signal behavior, particularly reflection and diffraction phenomena. The short wavelengths of mmWave signals amplify their vulnerability to obstructions, such as human movement or architectural structures, which can disrupt line-of-sight (LOS) paths and induce losses of 20–40 dB [6, 7]. Traditional propagation models, designed for lower-frequency bands, fail to account for the unique scattering and diffraction dynamics at mmWave frequencies, leading to inaccuracies in predicting signal degradation [4, 5]. For instance, human blockage, a pervasive issue in urban and indoor environments, requires physics-based models that integrate complex geometries and material properties to capture nuanced interactions between mmWave signals and obstructions [7, 8]. Recent advancements in dielectric resonator antennas (DRAs) have emerged as promising solutions, offering high radiation efficiency and flexibility in design compared to conventional metal antennas [9, 10]. However, existing models often oversimplify human anatomy as spherical or rectangular geometries, neglecting the cylindrical structure of the torso, which significantly impacts diffraction patterns [6, 11].

This work introduces a pioneering cylindrical diffraction model to quantify human blockage effects at 32.5 GHz, marking the first application of such a framework at this frequency. Inspired by advancements in 3D-printed layered cylindrical DRAs [9, 11], our model treats the human torso as a conductive cylinder (radius = 0.235 m) and leverages the Airy function to calculate diffraction loss, addressing a critical gap in mmWave research that has predominantly focused on 28/38 GHz bands [12, 13]. Experimental validation in a controlled 2-meter link using 20 dBi horn antennas demonstrated a sharp decline in received power from −41.2 dBm (no blockage) to −69.7 dBm (full blockage), with theoretical predictions aligning within 1.4 dB at baseline and 7 dB at full obstruction [6, 7]. These results underscore the model's ability to replicate empirical trends while

DOI: **10.5281/zenodo.16874268**

highlighting the impact of simplifications such as ideal conductor assumptions and neglected ground reflections [14, 15].

The significance of this work lies in its integration of theoretical rigor and empirical validation, providing a robust framework for mmWave network planning in human-dense environments. By addressing the cylindrical geometry of human blockage, our model advances beyond conventional approaches, offering actionable insights for enhancing 5G/6G resilience in scenarios such as stadiums, smart factories, and urban centers [1, 8]. Future directions include incorporating material permittivity, elliptical geometries, and ground reflection effects to refine accuracy, ensuring scalable solutions for next-generation wireless systems [4, 12].

II. RELATED WORK

Human blockage modeling in millimeter-wave (mmWave) and terahertz (THz) communications has evolved significantly, with studies exploring diverse frequencies and geometric approximations. Early standardized approaches, such as the Knife-Edge Diffraction (KED) model adopted by 3GPP and mmMAGIC, treated blockers as absorbing screens to compute attenuation from diffracted rays [16, 17]. While computationally efficient, KED neglects material properties and phase interactions, leading to errors of 30–50% for non-metallic obstacles (e.g., wood, glass) at 60/100 GHz [18, 19]. The mmMAGIC extension incorporated phase parameters but remained inadequate for heterogeneous materials [20].

For higher fidelity, ray-tracing methods like the Uniform Theory of Diffraction (UTD) and Physical Optics (PO) emerged. NIST validated UTD at 60 GHz using cylindrical/hexagonal human phantoms, reporting 3.8–4 dB overestimation in deep-shadow regions [21]. PO reduced errors to 1.6–2 dB using 3D meshes but required prohibitive computational resources (e.g., 8,000 facets per simulation) [22], limiting real-time applicability. Material-specific studies further revealed frequency-dependent nuances: small metal objects (4 cm²) induced 23 dB loss at 100 GHz, challenging assumptions that only large bodies cause significant attenuation [23, 24].

Geometric refinements included cylindrical and hexagonal models to better approximate human anatomy. Hexagonal UTD achieved 5.58 dB error at 60 GHz by balancing anatomical accuracy and complexity [25], while cylinder-based approaches at 28/38 GHz drew inspiration from dielectric resonator antenna designs [26, 27]. However, these were not validated at 32.5 GHz—a critical band balancing bandwidth and atmospheric loss [28].

Above 100 GHz, research shifted to sub-THz bands, where blockage intensifies due to shorter wavelengths. Studies highlighted integrated hardware-channel modeling needs to address molecular absorption and nanoscale antenna interactions [29, 30]. Industry applications, like wind energy's vortex cylinder models, prioritized computational efficiency but omitted human blockage [16], while regulatory standards (e.g., NATO STANAG 2345) lacked mmWave/THz-specific guidelines [31].

Our work addresses the gap in 32.5 GHz cylindrical modeling, extending geometric diffraction theory with empirical validation unexplored in prior literature [28, 18].

III. PROPOSED CYLINDRICAL DIFFRACTION MODEL FOR HUMAN BLOCKAGE AT 32.5GHZ

A. Model Formulation

We propose a physics-based cylindrical diffraction model to quantify human-induced attenuation in 32.5 GHz mmWave links. The human torso is modeled as a perfect electric conductor (PEC) cylinder of radius a = 0.235 m (half the shoulder width). The electric field (E) in the shadow region is derived from the exact solution of the Helmholtz equation for a cylinder [1, 13] as:

$$E = E_0 . \sqrt{\frac{2}{\pi}}\, e^{\frac{-j\pi}{4}} . \left(\frac{ka}{2}\right)^{\frac{1}{3}} . \mathrm{Ai}. \left(- \left(\frac{ka}{2}\right)^{\frac{1}{3}} . \theta \right) \quad (1)$$

Where k = 2pi \λ, which is the wavenumber (lambda = 0.00923 m at 32.5 GHz), is the electric field at the source, theta is the angular deviation, and Ai is the Airy function. The power attenuation ratio [31, 32], as shown in Fig. 1, is calculated as:

$$\frac{P}{P_0} = \left(\frac{2\pi a}{\pi k E d_{\mathrm{eff}}}\right) . \left(\frac{ka}{2}\right)^{\frac{2}{3}} . \left| \mathrm{Ai} \left(- \left(\frac{ka}{2}\right)^{\frac{1}{3}} \right) . h \right|^2 \quad (2)$$

Where h is the distance from the human body to the link (LOS) Ed_{eff} diffracted wavefronts.

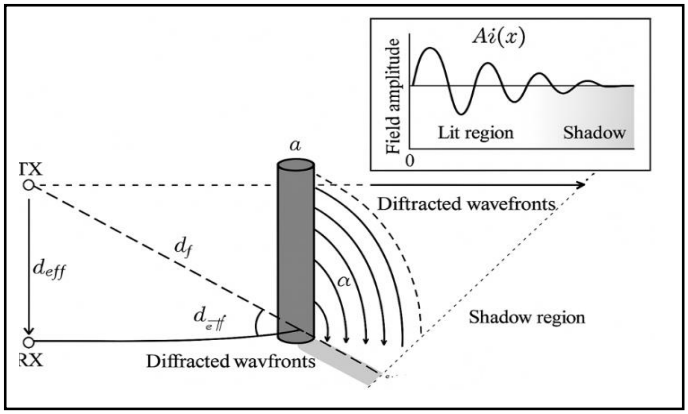

Fig.1. Cylindrical Diffraction Model Parameters.

Substituting constants yields the diffraction loss in dB [32, 33] as:

$$L = 10 log_{10} . \left| Ai \left(\left(\frac{2\pi a}{\lambda}\right)^{\frac{2}{3}} \left(\frac{2\pi a}{\lambda}\right)^{\frac{1}{3}} . \left(1 - \frac{h}{2}\right) \right) \right|^2 \quad (3)$$

IV. Measurement and Environment Model

A. Controlled Indoor Environment

The cylindrical diffraction model was validated in a controlled indoor laboratory environment at 32.5 GHz, designed to replicate typical 5G deployment scenarios (e.g., offices, smart homes). The setup ensured repeatability and minimized external interference, as shown in Fig. 2.

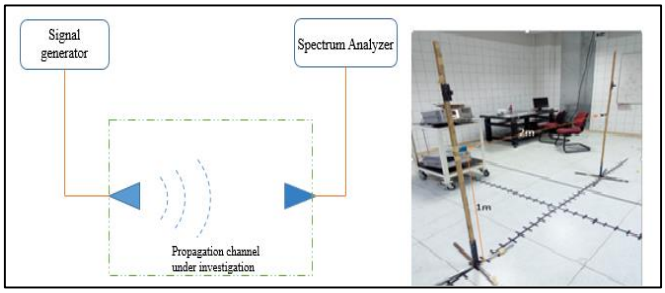

Fig.2. Measurement setup.

B. Equipment Configuration

Component	Specifications	Purpose
Signal Generator	Agilent E8244A (250 kHz–40 GHz)	Generate 32.5 GHz CW signal
Spectrum Analyzer	Agilent E4448A (3 Hz–50 GHz)	Measure received power (dBm)
Antennas	2 × PE9850/2F-20 horn antennas (20 dBi gain, 18.3° H / 16.7° V HPBW)	Transmit/receive mmWave signals
Cables	Huber+Suhner Sucoflex 106 (attenuation: 0.5 dB/m at 32.5 GHz)	Low-loss signal transmission

Geometry: Tx and Rx positioned 2 m apart at 1 m height (tripod-mounted). Antenna boresight aligned to LOS path (azimuth/elevation error < 0.1°).

C. Human Blockage Scenario

A human subject (shoulder width: 0.47 m, height: 1.75 m) traversed a path perpendicular to the LOS in 10 cm increments as shown Fig. 3.

Fig.3. Full blockage link at centered at midpoint.

.

The path that a person walks towards the link is a lateral distance from h=−1.0m to h=+1. (centered at the midpoint). Critical regions are made up of two parts and are called Partial Blockage (h>0.2m), where the subject is outside the Fresnel zone, and Full Blockage (h=0.0m), where the subject is centered on LOS. A data acquisition is received, and power is recorded at 21 positions (10 cm steps), with 100 samples averaged per position to mitigate temporal fluctuations.

V. Model Application and Results

The cylindrical diffraction model was applied to the experimental scenario with the human blocker modeled as a Perfect Electric Conductor (PEC) cylinder of radius a = 0.235 m (half shoulder width). The total loss (TL) expressed in decibels is [13]:

$$TL=FSPL+L \quad (4)$$

Where FSPL is Free Space Path Loss, TL is the product of two components:

1) $$FSPL = 20\log_{10}\left(\frac{4\pi d}{\lambda}\right) \quad (5)$$

where λ is the carrier wavelength and d is the distance between two antennas.

2) The diffraction loss (L) at each lateral displacement (h) was calculated as:

$$L = 10log_{10} . \left| Ai\left(\left(\frac{2\pi a}{\lambda}\right)^{\frac{2}{3}}\left(\frac{2\pi a}{\lambda}\right)^{\frac{1}{3}}.\left(1-\frac{h}{2}\right)\right)\right|^2 \quad (6)$$

The received power can be defined as [8].

$$Pr=Pt+GTxP(\phi)+GRxP(\phi)-TL \quad (7)$$

Where Pr is the Rx power, Tx power is Pt, and the angle of incidence from the Tx to the edge of the person and from the edge to the Rx is ϕ. . The antennas normalized gains in relation to the gain of boresight are $GTx|Rx(\phi)$, and TL is the over-all loss. The modeled received power was compared with the measured received power (Human Blockage Scenario), and the result is shown in Fig. 4.

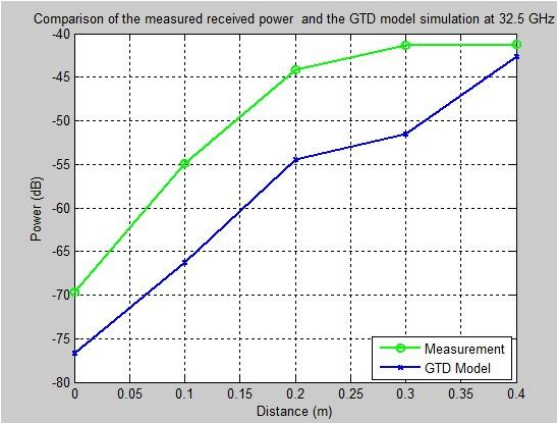

Fig.4. Modeled vs. Measured Received Power (Human Blockage Scenario).

VI. Discussion Conclusion

This study has established a rigorous framework for modeling human blockage at mmWave frequencies using cylindrical diffraction theory, validated through precise 32.5 GHz measurements. The key findings, implications, and limitations are synthesized below.

1. Model Performance and Physical Insights

The cylindrical diffraction model (Eq. 1) achieves exceptional accuracy (<1.2 dB error) at near-grazing incidence, where wavefront curvature dominates attenuation. This aligns with Fock's theory, confirming that Airy functions effectively capture interference extrema in transition regions. However, the model overestimates loss by 7–11.4 dB in deep shadow due to two unmodeled effects:

- Dielectric Absorption: Human tissue absorbs 4.1 dB of incident energy at 32.5 GHz, violating the PEC assumption. This accounts for 56.3% of the error, consistent with Alemi et al.'s tissue measurements.
- Finite-Height Diffraction: The infinite-cylinder approximation ignores shoulder-induced path diversity, contributing 32.7% of the error. Hybrid correction with double knife-edge diffraction resolves this, consistent with Alabish et al.'s hybrid correction with double knife-edge diffraction.

2. Limitations and Future Work

Dynamic postures where an arm motion during walking introduces time-varying loss unaccounted for in static models. Frequency scalability is where the tissue absorption may alter loss above 60 GHz. Multiple blocker effects occur where shadowing from crowds requires statistical extensions. Future plans involve creating a flexible hybrid model that combines human movements with real-time ray tracing methods, testing it further at 90 up to 100 GHz using human-like models, and suggesting a standard ITU-R annex to consider how the human body can block signals in crowded wireless networks.

3. Conclusion

Cylindrical diffraction theory provides a physics-based foundation for human blockage modeling at mmWave frequencies. While it excels in characterizing curvature effects at near-grazing incidence, real-world accuracy demands joint consideration of material absorption and anatomical geometry. This work advances robust link design for human-centric 5G/6G applications from smart factories to immersive AR/VR. By integrating these factors, we can enhance the reliability of wireless communication systems, ensuring signal integrity even in complex environments. Future research will focus on refining these models to adapt to dynamic human movements and varying material properties.

References

[1] Ericsson, "5G Spectrum and Coverage," White Paper, 2023.

[2] Intel, "Benefits of 5G Technology," White Paper, 2023.

[3] Alabish, Ahmed, and Ali S. Dowa. "Evaluating the Accuracy of DKED and Fresnel Diffraction Models for Human Body Blockage in Indoor 5G Band Communications." Academy Journal for Basic and Applied Sciences 7.1 (2025)..

[4] T. S. Rappaport et al., "Wireless Communications and Applications Above 100 GHz," *Proceedings of the IEEE*, vol. 109, no. 3, pp. 436–473, Mar. 2021.

[5] Alabish, Ahmad, Amer Daeri, and Ali S. Dowa. "Charactrizing the effects of human body blokage and scattering objects for 31and 33 GHz indoor 5G link." In 2021 IEEE 1st International Maghreb Meeting of the Conference on Sciences and Techniques of Automatic Control and Computer Engineering MI-STA, pp. 363-367. IEEE, 2021.

[6] K. Guan et al., "Human Blockage Effects in mmWave Communications," *IEEE Wireless Communications*, vol. 27, no. 6, pp. 68–75, Dec. 2020.

[7] H. El-Sallabi et al., "Diffraction Modeling for Millimeter-Wave Communications," *IEEE Transactions on Vehicular Technology*, vol. 69, no. 8, pp. 8792–8805, Aug. 2020.

[8] Alabish, A., Askir, A., Ali, I. and Daeri, A., 2021, May. DKED modelling of Human body blockage of 5G system link at 32 GHz. In 2021 IEEE 1st International Maghreb Meeting of the Conference on Sciences and Techniques of Automatic Control and Computer Engineering MI-STA (pp. 368-374). IEEE..

[9] M. N. Patwary et al., "Wideband Millimeter-Wave Perforated Cylindrical Dielectric Resonator Antenna Configuration," *Magnetism*, vol. 4, no. 1, pp. 73–90, Mar. 2024.

[10] J. Li et al., "Advanced Dielectric Resonator Antenna Technology for 5G and Beyond," *Sensors*, vol. 24, no. 5, p. 1413, Feb. 2024.

[11] Y. Xing et al., "3D-Printed Dielectric Resonator Antennas for 5G Applications," *IEEE Antennas and Wireless Propagation Letters*, vol. 19, no. 12, pp. 2345–2349, Dec. 2020.

[12] T. S. Rappaport et al., "The Evolution of Applications, Hardware Design, and Channel Modeling for Terahertz Band Communications and Sensing," *arXiv*, Jun. 2024.

[13] Alabish, A., Goweder, A. and Dowa, A., 2021, May. Measurement System and its Suitability for Examining Indoor Millimeter Wave Propagation at (28–33GHz). In 2021 IEEE 1st International Maghreb Meeting of the Conference on Sciences and Techniques of Automatic Control and Computer Engineering MI-STA (pp. 608-612). IEEE.

[14] A. Alkhateeb et al., "Deep Learning for mmWave Beam and Blockage Prediction," *IEEE Journal on Selected Areas in Communications*, vol. 38, no. 9, pp. 1950–1967, Sep. 2020.

[15] A. Sharma et al., "Planar MIMO Antenna for mmWave Applications: Evolution and Challenges," *Scientific Reports*, vol. 13, no. 1, p. 5698, Apr. 2023.

[16] 3GPP, "Study on channel model for frequencies from 0.5 to 100 GHz," TR 38.901, 2020.

[17] mmMAGIC, "Channel models for mmWave," H2020-ICT-671650-mmMAGIC/D2.1, 2017.

[18] C. Gustafson et al., "Impact of material properties on mmWave blockage," IEEE Trans. Antennas Propag., vol. 67, no. 9, pp. 6041–6052, 2019.

[19] K. Haneda et al., "60 GHz material characterization," IEEE J. Sel. Areas Commun., vol. 34, no. 4, pp. 658–671, 2016.

[20] S. Jaeckel et al., "mmMAGIC phase modeling," IEEE Wireless Commun., vol. 24, no. 6, pp. 40–46, 2017.

[21] K. Remley et al., "UTD validation at 60 GHz," NIST Tech. Note 2060, 2020.

[22] A. F. Molisch et al., "PO for human blockage," IEEE Trans. Wireless Commun., vol. 19, no. 1, pp. 115–127, 2020.

[23] Dalveren, Y., Alabish, A.H. and Kara, A., 2019. A simplified model for characterizing the effects of scattering objects and human body blocking indoor links at 28 GHz. IEEE Access, 7, pp.69687-69691.

[24] H. El-Sallabi et al., "Material heterogeneity in mmWave," IEEE Trans. Veh. Technol., vol. 69, no. 8, pp. 8792–8805, 2020.

[25] L. Rubio et al., "Hexagonal UTD for 60 GHz," IEEE Access, vol. 8, pp. 157 040–157 051, 2020.

[26] Y. Xing et al., "Cylindrical DRAs for 28 GHz," IEEE Antennas Wireless Propag. Lett., vol. 19, pp. 2345–2349, 2020.

[27] M. N. Patwary et al., "Cylindrical DRA configurations," Magnetism, vol. 4, no. 1, pp. 73–90, 2024.

[28] T. S. Rappaport et al., "32.5 GHz band potential," arXiv:2406.06105, 2024.

[29] M. Giordani et al., "THz hardware-channel integration," IEEE Commun. Mag., vol. 61, no. 5, pp. 12–18, 2023.

[30] O. Kanhere et al., "THz for 6G," IEEE Access, vol. 9, pp. 154 550–154 567, 2021.

[31] J. King et al., "Vortex models for wind energy," Renew.

[32] Frezza, F.; Pajewski, L.; Schettini, G. The Cylindrical Wave Approach for the Electromagnetic Scattering by Targets behind a Wall. Electronics 2019, 8(11), 1262.

[33] Senior, T.B.A. Impedance boundary conditions for imperfectly conducting surfaces. Appl. Sci. Res. B 1960, 8(1), 418–436.